Use of Strain in a Stereospecific Catalytic Mechanism: Crystal Structures of *Escherichia coli* Thymidylate Synthase Bound to FdUMP and Methylenetetrahydrofolate[†,‡]

David C. Hyatt,[§] Frank Maley,[||] and William R. Montfort*[,§]

Department of Biochemistry, University of Arizona, Tucson, Arizona 85721, and Wadsworth Center, New York State Department of Health, Albany, New York 12201-0509

Received December 2, 1996; Revised Manuscript Received February 10, 1997[⊗]

ABSTRACT: Two crystal structures for *E. coli* thymidylate synthase (TS) bound to the mechanism-based inhibitor 5-fluoro-dUMP (FdUMP) and methylenetetrahydrofolate (CH_2THF) have been determined to 2.6 and 2.2 Å nominal resolutions, with crystallographic *R* factors of 0.180 and 0.178, respectively. The inhibitor and cofactor are well ordered in both structures and display covalent links to each other and to Cys 146 in the TS active site. The structures are in general agreement with a previous report for this complex (D. A. Matthews et al. (1990) *J. Mol. Biol. 214*, 937−948), but differ in two key respects: (i) the methylene bridge linking FdUMP and CH_2THF is rotated about 60° to a different position and (ii) the electron density for C6 of FdUMP, which is covalently linked to Cys 146, is more diffuse than for the other atoms in the pyrimidine ring. The ligand arrangement observed in the previous structure led the authors to propose that a large conformational change in ligand geometry must occur in order to facilitate catalysis and yield the correct chirality in the methyl of product dTMP. The new structures suggest a different mechanism for product formation that does not require ligands to greatly alter their conformations during catalysis and which makes use of instability in the nucleotide−Cys 146 thiol adduct to avoid a deep free energy well and assist in proton abstraction from dUMP. All intermediates in the proposed mechanism were modeled and energy minimized in the TS active site, and all can be accommodated in the present structures. The role of ligand-induced conformational change in the TS mechanism and the possibility of Tyr 94 acting as a base during catalysis are also discussed.

Thymidylate synthase (TS)[1] has long been studied as a target for antiproliferative agents due to its central role in DNA synthesis and for its rich mechanistic features [reviewed in Pogolotti and Santi (1977), Santi and Danenberg (1984), Carreras and Santi (1995), and Hardy (1995)]. TS catalyzes the reductive methylation of dUMP to dTMP using the cofactor methylenetetrahydrofolate (CH_2THF) and provides the sole *de novo* means for synthesizing dTMP. Compounds modeled after both substrate and cofactor have been studied as potential inhibitors of TS. 5-Fluorouracil, which is metabolically converted to 5-fluoro-dUMP (FdUMP), is a long-standing chemotherapeutic agent that acts to inhibit TS *in vivo*. More recently, analogues of CH_2THF have been designed that show promise as anticancer drugs (Smith et al., 1995, 1996; Webber et al., 1996). Studies leading to the design of these inhibitors have resulted in a wealth of biochemical and structural data and a proposed catalytic mechanism, shown in Figure 1.

The conclusions from the structural work to date have not been consistent with the mechanism predicted from solution studies or with the known stereochemistry of the TS reaction (Pogolotti & Santi, 1977; Tatum et al., 1977; Sliecker & Benkovic, 1984). Specifically, it was observed that when (6*R*,11*S*)-5,10-methylene[11-^{2}H,^{3}H]tetrahydrofolate is used as cofactor, the resulting product is (*S*)-methyl[*methyl*-^{1}H,^{2}H,^{3}H]dTMP (Sliecker & Benkovic, 1984). The inconsistency arises from the predicted conformation of intermediate **III** (Figure 1) from structural studies and its proposed mechanism of breakdown, which leads to an *R* configuration for the methyl group of the product. The structure of the covalent ternary complex TS·FdUMP·CH_2THF (Matthews et al., 1990b), which is thought to be very similar to intermediate **III**, revealed a ligand geometry such that hydride transfer would occur to the wrong side of the methylene group. A similar conclusion was reached from modeling of intermediate **III** based on the structure of TS·dUMP·CB3717, where CB3717 is a tightly-binding folyl analogue (Finer-Moore et al., 1990). A second difficulty revealed by these structures was the equatorial position of the pyrimidine C5 fluorine. This arrangement has been observed both crystallographically and by fluorine NMR (Byrd et al., 1978). In the reaction with dUMP, the proton at this position is removed and has been argued to be less acidic in an equatorial position than it would be in an axial position (Matthews et al., 1990b; Finer-Moore et al., 1990).

[†] This work was supported in part by American Cancer Society grant DHP-45 (W.R.M.) and National Cancer Institute Grant CA44355, USPHS/HHS (F.M.).

[‡] The final coordinates for the trigonal and hexagonal crystal forms have been deposited with the Brookhaven Protein Data Bank (entry numbers 1tsn and 1tls, respectively).

* Corresponding author: William R. Montfort, Dept of Biochemistry, University of Arizona, Tucson, AZ 85721. Tel. (520) 621-1884; Fax (520) 621-1697; e-mail montfort@biosci.arizona.edu.

[§] University of Arizona.

[||] Wadsworth Center.

[⊗] Abstract published in *Advance ACS Abstracts,* March 15, 1997.

[1] Abbreviations: TS, thymidylate synthase; CH_2THF, 5,10-methylenetetrahydrofolate; THF, 5,6,7,8-tetrahydrofolate; DHF, 7,8-dihydrofolate; FdUMP 5-fluoro-dUMP.

S0006-2960(96)02936-4 CCC: $14.00

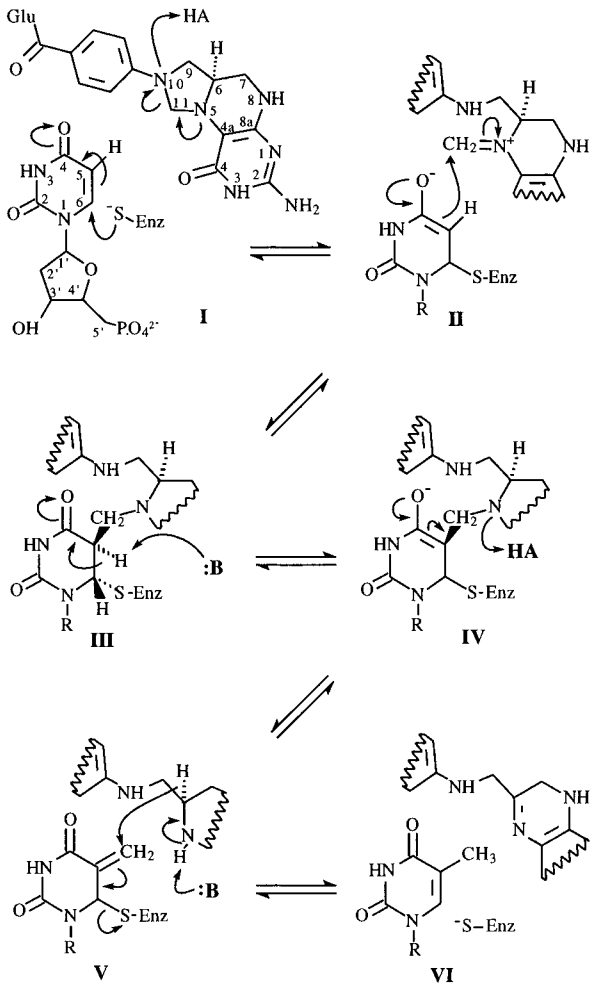

FIGURE 1: General features of the TS catalytic mechanism (Pogolotti & Santi, 1977; Santi & Danenberg, 1984; Carreras & Santi, 1995).

A third difficulty noted by Matthews et al. was that the Cys 146 sulfur, which is in an axial position, would be a better leaving group than tetrahydrofolate (THF) and would eliminate to produce the original starting materials.

On the basis of these considerations, Matthews and coworkers proposed that the covalently linked intermediate **III** must undergo an extensive isomerization before breakdown of the complex. This proposal was attractive because it addressed all of the difficulties described above. First, the isomerization would rotate the methylene bridge so that hydride transfer would occur at the opposite face, giving the experimentally observed stereochemistry. Second, the isomerization would place the pyrimidine C5 proton in an axial position, where it could more easily be removed. Finally, the proposed isomerization would place the Cys 146 sulfur in an equatorial position, which would favor the elimination of THF. Support for the isomerization comes from NMR studies of the covalently linked complex TS·FdUMP·CH_2-THF after denaturation and proteolysis (James et al., 1976).

Since the above studies were completed, crystal structures of TS bound to a variety of ligands have been determined. These studies confirm that TS undergoes an extensive conformational change during catalysis (Matthews et al., 1990b; Montfort et al., 1990), but it did not appear to us that any of the observed conformations of the enzyme would accommodate the proposed ligand isomerization. We therefore reinvestigated the structure of TS·FdUMP·CH_2THF in an attempt to resolve this issue and clarify the role of enzyme conformational change in the catalyzed reaction. Crystal structures were determined for the complex with *E. coli* TS in two space groups, $P6_3$ and $P3_121$, to nominal resolutions of 2.6 and 2.2 Å, respectively. The structure previously reported (Matthews et al., 1990b) was in space group $P6_1$ at 2.5 Å nominal resolution. The new structures are in general agreement with the previous one except for two differences. First, the position of the methylene bridge linking FdUMP and CH_2THF is slightly rotated, with the C11−N5 bond *gauche* to the C5−F bond, very similar to the model predicted from the TS·dUMP·CB3717 structure (Finer-Moore et al., 1990). Second, the density for C6 of FdUMP, where Cys 146 becomes covalently attached, is much worse than for the other atoms in the ring. On the basis of these observations, coupled with our modeling studies, we propose a mechanism for the breakdown of the covalent ternary complex that yields the correct stereochemistry without resorting to major changes in conformation of either ligands or protein. Our proposed mechanism follows a path different from the predominant path expected in the absence of protein. To accomplish this, we suggest that TS makes use of strain, electrostatic interactions, and conformational change to influence the reaction along a more conformationally restricted path.

MATERIALS AND METHODS

Crystallization. Crystals were grown by the hanging drop vapor diffusion method. Protein was overexpressed and purified as previously described (Maley & Maley, 1988). (6*R*,*S*)-CH_2THF was prepared from purified folic acid, as described (Galivan et al., 1976a). (6*S*)-CH_2THF is a weak competitive inhibitor of TS [$K_i = \sim 50$ μM for the *L. casei* enzyme (Leary et al., 1974)]. However (6*R*)-CH_2THF forms a covalently-linked ternary complex with TS and FdUMP that results in ~50000-fold tighter binding of FdUMP than occurs with the (6*S*) isomer (Galivan et al., 1976a; Santi et al., 1974). No indication of binding by the (6*S*) isomer was detected in the present crystal structures. For growing crystals of the $P6_3$ space group, drops were prepared from a solution containing *E. coli* TS (8 mg/mL), FdUMP (2 mM), (6*R*,*S*)-CH_2THF (~1 mM), phosphate (20 mM, pH 7.5), DTT (4 mM), and ammonium sulfate (1.05 M). Five microliters of this solution was equilibrated against a solution containing phosphate (20 mM, pH 7.5), DTT (4 mM), and 2.1 M ammonium sulfate. Crystals of the $P3_121$ space group grew under identical conditions, but were of better quality when grown at pH 8.0 and at slightly higher ammonium sulfate concentrations. Crystals appeared within 48 h and continued growing for several days.

Structure Determination. A single data set was collected from each of the two crystal forms. The $P3_121$ crystal was approximately 0.3 × 0.4 mm and diffracted to a nominal resolution of 2.2 Å. The $P6_3$ crystal was approximately 0.4 × 0.2 mm and diffracted to a nominal resolution of 2.6 Å. Diffraction data were measured using an Enraf Nonius FAST area detecting diffractometer attached to a FR571 rotating Cu anode X-ray source. Data reduction was performed using the software package MADNES (Messerschmidt & Pflugrath, 1987) and PROCOR (Kabsch, 1988). Refinement was performed with GPRLSA (Furey et al., 1982), using observed structure factor amplitudes and starting phases from isomorphous crystals of similar complexes ($P3_121$ and $P6_3$ forms

of TS·FdUMP·CB3717 (Hyatt & Montfort, unpublished results)). Structure factors and electron density maps were calculated using the CCP4 program suite (Collaborative Computational Project, 1994). Model building was performed using FRODO (Jones, 1978; Pflugrath et al., 1984).

Modeling. Intermediates **I**, **II**, **IV**, and **V** were built and energy minimized using the Insight II/Discover software package (Insight II, 1993). The intermediates were constrained to have conformations similar to those observed for FdUMP and CH_2THF in the present structures, and all but intermediate **I** had a cysteine covalently linked to C6 of the pyrimidine ring (1.85 Å). The models were then placed into a subset of the TS 2.2 Å trigonal structure that consisted of all amino acids and ordered water molecules that contacted ligands (37 residues and 12 water molecules in all). This model was then subjected to additional energy minimization where the protein, the ordered solvent molecules, and one atom from each ligand (the phosphate of dUMP and one atom in the THF pterin ring) were fixed and the remaining ligand atoms were allowed to move. The two atoms in the ligands were fixed to prevent the ligands from moving away from the known binding positions (bulk solvent was not included), and the fixed atoms were varied to avoid systematic errors. The Cff91 parameter file was used to assign potentials. Each complex was refined to convergence and resulted in models with reasonable geometry for the ligands and no steric conflicts between protein and ligand.

RESULTS AND DISCUSSION

Structures of TS·FdUMP·CH_2THF. To resolve the issues concerning the mechanism for breakdown of the covalent ternary complex (intermediate **III**) and the observed product stereochemistry, the structure of TS·FdUMP.·CH_2THF was determined in two space groups, $P3_121$ and $P6_3$, to nominal resolutions of 2.2 and 2.6 Å, respectively. Both crystal forms were isomorphous with crystals of TS·FdUMP·CB3717 previously determined in the same two space groups (Hyatt & Montfort, unpublished results), and the TS·FdUMP·CB3717 models provided the initial coordinates for the present structures. TS is a functional dimer and is present as such in all crystals examined to date. The $P3_121$ crystal contained a monomer in the asymmetric unit with the two halves of the dimer related by a crystallographic dyad, while the $P6_3$ crystal contained the full dimer in the asymmetric unit. Thus three views of the new complex were available to us, two from the $P6_3$ crystals and one from the $P3_121$ crystals.

Difference electron density maps calculated with F_{obs} and phases from the starting models revealed a shift in the CH_2THF position relative to that of CB3717. The major peaks in these maps were similar for all three views of the TS active site. Large positive and negative peaks on either side of the pterin and PABA rings indicated that, in the CH_2THF containing complex, the pterin ring was shifted closer to FdUMP and slightly rotated. A positive peak between the CH_2THF and FdUMP moities, averaging 13σ in the three active sites, was consistent with methylene bridge formation between the two groups. A negative peak coinciding with the position of the CB3717 propargyl group, which is not present in CH_2THF, was also apparent in the map and averaged 11σ. Difference electron density for the thiol adduct between Cys 146 and C6 of the FdUMP pyrimidine ring was more difficult to interpret. In the CB3717 containing complex, the thiol adduct is present in both active sites of the $P6_3$ crystal structure, although a little weak in one active site, while this bond is absent in the $P3_121$ complex. The difference electron density maps between the CB3717 and CH_2THF crystals indicate a slight shift in the pyrimidine ring position, indicate a slight rotation of the Cys 146 sulfur, and are consistent with partial covalent bond formation (see below).

Table 1. Crystallographic Data

space group	$P3_121$	$P6_3$
cell constants (Å)	$a = 72.10$	$a = 126.78$
	$c = 115.27$	$c = 67.71$
resolution (Å)	2.2	2.6
total reflections	76346	63040
unique reflections	18104	18880
% total data	98.4	99.5
R_{sym} (all data)[a]		
total/outer shell	0.095/0.36	0.10/0.43
av $I/\sigma(I)$		
total/outer shell	12.6/1.9	15.1/1.0
RMS deviations		
bond distances (Å)	0.019	0.017
bond angles (deg)	3.0	2.5
R_{cryst} (all non-zero data)	0.178	0.180
av temp factors (Å^2)		
protein atoms		
monomer 1	21.3	14.6
monomer 2		20.3
ligand atoms		
monomer 1	22.0	22.6
monomer 2		27.6

[a] Data were truncated at the resolution where the percentage of $I > 3\sigma(I)$ fell below 33%.

Initial models for the new complex were built into $F_o - F_c$ "omit" electron density maps, where the ligands were removed from the model before calculating structure factors. The positions for all atoms were clearly indicated in these maps. Refinement was initially performed with the distance between the Cys 146 sulfur and C6 of FdUMP restrained to 1.85 Å (the usual distance for such bonds) but later to 2.1 Å to achieve a better fit with the observed electron density (see below). Final statistics for data collection and model refinement are shown in Table 1. A ribbon diagram indicating ligand position for one monomer is shown in Figure 2, and the final electron density for ligands is shown in Figure 3.

The final TS·FdUMP·CH_2THF models are very similar to one another and to the CB3717-containing structures. The RMS deviations between Cα atoms for the $P3_121$ CH_2THF complex and each of the two active sites of the $P6_3$ CH_2THF complex are 0.28 Å in both cases, and the RMS deviations between the CH_2THF and CB3717 structures are 0.14 and 0.12 Å, respectively, for the $P3_121$ and $P6_3$ crystal forms. The only significant differences between the CB3717- and CH_2THF-containing structures are in the active site, where residues in contact with CH_2THF shift slightly to accommodate the absence of a propargyl group and the slight changes in position for the ligands. Part of the gap created by removal of the propargyl group is filled with a new water molecule that hydrogen bonds to both N10 of CH_2THF (2.8 Å) and Oε of Glu 58 (3.0 Å).

Unexpected Ligand Arrangements. The resulting model for ligands, shown in Figure 4, is similar to that previously reported by Matthews and co-workers (1990b). The C11−

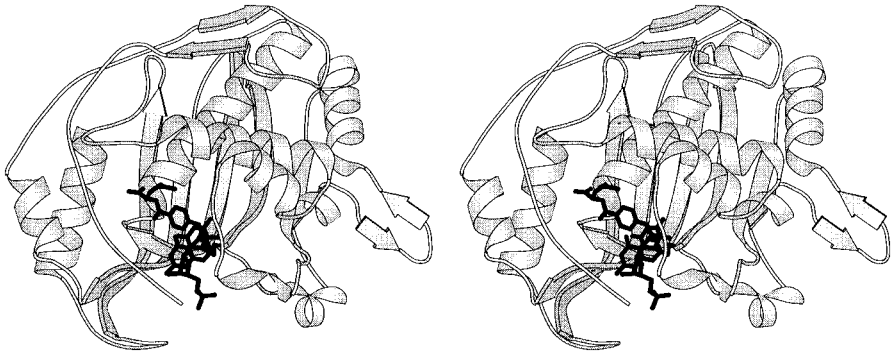

FIGURE 2: Stereoribbon diagram showing a TS monomer from *E. coli* in a complex with FdUMP and CH_2THF (shown in black). This figure, Figure 4, and Figure 6 were produced with the program MOLSCRIPT (Kraulis, 1991).

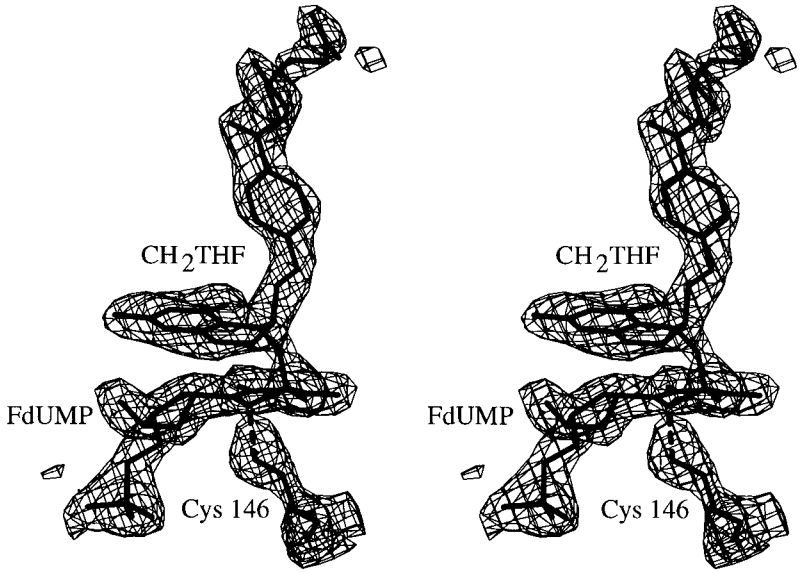

FIGURE 3: Stereoview of electron density for ligands and Cys 146 in the TS·FdUMP·CH_2THF ternary complex. The electron density is from the final $2F_o - F_c$ map for the trigonal crystal form and is contoured at 2σ above the mean value for the entire map. This figure and Figure 5 were produced with the program O (Jones et al., 1991).

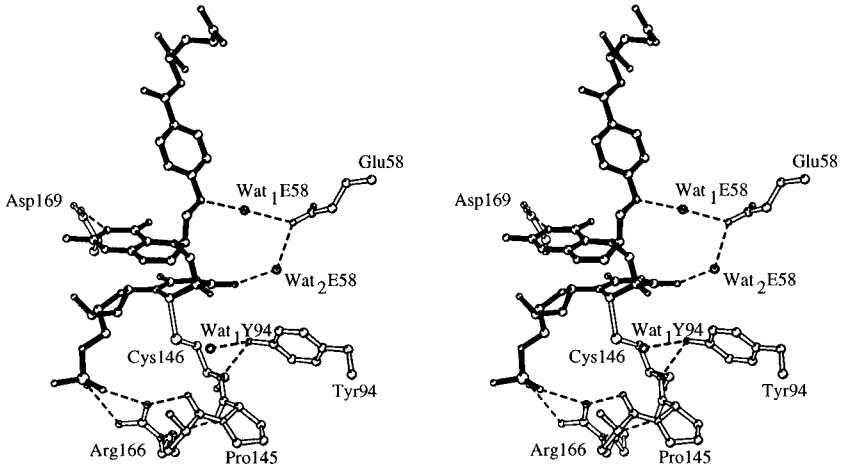

FIGURE 4: Stereoview of the active site region and the bound FdUMP·CH_2THF complex. Protein atoms are indicated by white bonds, ligand atoms by black bonds, water molecules by open circles, and hydrogen bonds by dashed lines. Nitrogen and oxygen atoms are drawn smaller than carbons and phosphates drawn larger. The N5−C11 bond is oriented *gauche* with respect to the C5−F bond, and a new ordered water molecule, Wat_1E58, is hydrogen bonded to both the side chain of Glu 58 and N10 of CH_2THF.

C5 methylene bridge between CH_2THF and FdUMP lies axial to the pyrimidine ring, and the fluorine lies in a pseudoequatorial position. The thiol linkage between Cys 146 and C6 of FdUMP is also axial. However our model differs from the earlier structure in one key respect: N5 is rotated about the C5−C11 bond by ~60° from the previously reported structure, to a conformation that is *gauche* with respect to the C5 substituents. All three active sites reported here display this arrangement. In the previously reported structure, the N5−C11 bond lies above the C5−F bond in a synperiplanar arrangement.

A second surprising result is that the electron density for C6 and the C6−Cys 146 bond is considerably weaker than for the rest of the ligand atoms and thus has been indicated

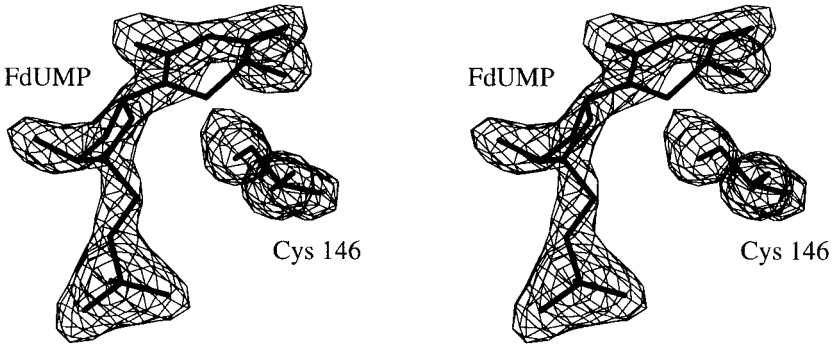

FIGURE 5: Difference (F_o - F_c) electron density where FdUMP and Cys 146 atoms where omitted from the calculated structure factors. The map is contoured at 8σ above the mean value for the entire map. At this contour level, electron density for C6 is absent, while density for the other atoms in FdUMP and Cys 146 is well defined.

with a dashed line in Figure 3. The missing density is more apparent in maps contoured at higher density, as shown in Figure 5. Poor density for C6 has been noted in other complexes (Weichsel & Montfort, unpublished results), as well as variablility in the covalent linkage between C6 and Cys 146 (Weichsel & Montfort, 1995; Matthews et al., 1990a). On the basis of this and other factors, we suggest below that the poor density seen in the present structures for C6 results from a mixed population of covalently linked and unlinked FdUMP molecules in the crystal and that the observed instability of the thiol adduct is a necessary feature for catalysis by TS.

Modeling of Other Intermediates. The new crystal structures present a close analogue of intermediate **III** from Figure 1. As described in the introduction, there was an inconsistency between the previous model for this intermediate and the known stereochemistry of the product. We sought to determine if the new position for the methylene bridge could help resolve this issue, as well as provide insight into other steps in the TS mechanism. To accomplish this, we modeled intermediates **I, II, IV,** and **V** from Figure 1. Intermediate **VI**, the product complex, has already been determined for the wild type (Weichsel & Montfort, unpublished results) and the C146S mutant protein (Fauman et al., 1994).

In our modeling we first assumed the protein conformation was unchanged from that of the present structures. TS undergoes a ligand-induced conformational change upon ternary complex formation (Montfort et al., 1990; Matthews et al., 1990b), which raises the possibility that one or more additional protein conformations may occur to accommodate the intermediates under study. Considerable structural data now exist which suggest that only one overall protein conformation occurs in TS ternary complexes. For example, as observed in the present work, identical ternary complexes crystallized in different space groups give rise to the same protein conformation. Structures exhibiting intermediate positions along the continuum from open to closed have been observed (Weichsel & Montfort, unpublished results), but no conformations that significantly deviate from this path have been discovered to date. Even upon ternary complex formation with BW1843, an analogue of CH_2THF that induces a local distortion in the active site upon binding, the overall ligand-induced conformation of the protein is similar to that of the present study (Stout & Stroud, 1996; Weichsel & Montfort, 1995; Weichsel et al., 1995). Thus, we investigated whether this protein conformation could accommodate the remaining proposed intermediates.

Each of the intermediates was built and energy minimized to yield acceptable stereochemistry while restrained in a conformation similar to that of CH_2THF in the present structures (see Methods for details). The intermediate was then placed in the TS active site and further minimized while keeping the protein and certain well-ordered water molecules fixed in place. The next few sections detail the results of these minimizations. To anticipate our conclusions, we found that the closed TS conformation, as seen in the present structures, is able to accommodate all intermediates in a stepwise-elimination mechanism that gives rise to the correct stereochemistry, while a mechanism requiring a shift in the Cys 146−dUMP covalent bond from an axial to an equatorial position is not consistent with any known conformation of the protein. The resulting ligand conformations are shown in Figure 6.

Cofactor Binding and Activation. The key difficulty in modeling the noncovalently linked ternary complex (intermediate **I**) lies in the conformation of CH_2THF, as was extensively discussed by Matthews et al. (1990b). The unbound conformation for CH_2THF, as determined by X-ray diffraction (Tamelen & Hopla, 1979) and NMR (Poe et al., 1979) approaches, is relatively flat with the PABA ring extended away from the pterin ring. This conformation is unlike the bent conformation of TS-bound folates and will not fit in any of the known conformations of the TS active site. However a bent conformation nearly identical to that for THF in the present structure can be reached through increased pyrimidylization of N10, and by rotating atoms attached to C6 and C7 from axial to equatorial positions. Such a model places the PABA ring above the pterin ring and will fit into the TS active site without any adjustment in the positions of protein atoms.

Shown in Figure 6 is the model for intermediate **I** with CH_2THF in the bent conformation, after energy minimization in the TS active site. This conformation retains all of the protein−ligand contacts formed by THF in the TS·FdUMP·CH_2THF structures. It has been argued that the five-membered imidazolidine ring is strained in the bent conformation (Poe et al., 1979); however our model does not appear to be so high in energy that it could not be stabilized in the enzyme complex.

We suggest that only the bent conformation of the cofactor forms a tightly-bound complex with the enzyme and nucleotide [binding of CH_2THF does not occur in the absence of nucleotide (Galivan et al., 1976b), unless polyglutamylated (Lu et al., 1984)]. The extended conformation may be able to form a loosely-bound ternary complex with the open TS

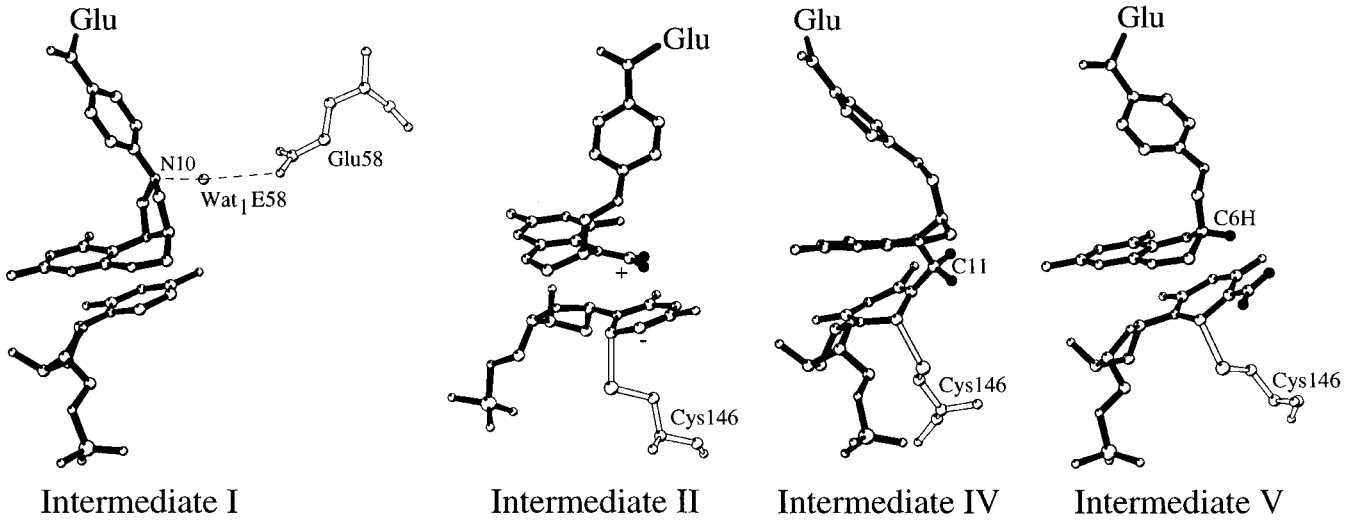

FIGURE 6: Energy-minimized models for intermediates along the TS-catalyzed reaction pathway. Ligands are shown with black bonds, protein atoms with white bonds, and selected hydrogen atoms with filled balls. The position of the folyl glutamate is indicated by "Glu". Numbering of intermediates is as in Figure 1.

conformation through nonspecific electrostatic and hydrophobic interactions, which would raise the local concentration of cofactor near the active site. Adoption of the bent conformation by CH_2THF would allow tight binding to the protein−nucleotide binary complex and induce closure of the active site. The energy to accomplish this could come from the extensive binding interactions between the protein and ligands that occur only in the closed conformation. Thus, one role for the TS ligand-induced conformational change may be to stabilize the higher energy bent conformer of CH_2THF that is required for catalysis by completely surrounding it, while providing only a nonspecific, more open binding surface for the extended conformer.

Once bound, it is thought that the imidazolidine ring of the cofactor opens to form an iminium ion (intermediate **II**) at N5 (Kallen & Jencks, 1966). Formation of this intermediate requires the protonation of N10, and it has been proposed that invariant Glu 58 is involved in this step (Matthews et al., 1990b; Zapf et al., 1993). Our present structures show a well-ordered water molecule within hydrogen-bonding distance of both Glu 58 and N10 of the cofactor, and in perfect alignment for protonation of N10 (Wat_1E58[2] in Figure 4). Whether E58 is the ultimate proton source for ring opening, or simply serves to order the appropriate water molecules, is unclear at present.

The possibility that ring opening and methylene bridge formation between dUMP and CH_2THF could "proceed through a concerted bimolecular substitution mechanism in which formation of the free imminium ion is circumvented" has recently been suggested (Eldin & Jenks, 1996). In such a mechanism, intermediate **II** would not occur, but the water molecule near N10 would still be employed. The ligand arrangement in our model for intermediate **I** has C5 and C11 aligned such that a concerted mechanism could occur.

Covalent Ternary Complex Formation. Our model for intermediate **II** (Figure 6) is nearly identical to the ligands in the present structure except for the position of C11. In the model, N5 is sp^2 hybridized and the 5-iminium group is planar with the pterin rings. C11 lies directly above C5 of dUMP and is perfectly aligned for nucleophilic attack by the pyrimidine C5 carbanion. The C11 protons and N5 are staggered with respect to C4, C5H, and C6. Nucleophillic attack by C5 on C11 would yield intermediate **III** in a conformation nearly identical to that of the present structures. Both N5 of CH_2THF and C5 of dUMP undergo rehybridizations from sp^2 to sp^3 during the reaction.

Elimination Step 1: Proton Abstraction from the Pseudoequatorial Ring Position. The heart of our model concerns the elimination of the dUMP C5 proton and THF. E2 eliminations proceed with the orbitals of the leaving groups aligned in either a syn- or antiperiplanar arrangement. In the structure reported by Matthews and co-workers (1990b), C5H and THF were aligned approximately synperiplanar. Although this alignment is appropriate for an E2 elimination of THF, it would give rise to incorrect stereochemistry of the methyl group if the reaction proceeded directly. As described in the introduction, they suggested that the ligands must undergo a change in conformation that would place the C5 and C6 hydrogens of dUMP trans-diaxial, create an antiperiplanar arrangement for C5H and C11, and switch the C6−Cys 146 adduct from an axial to an equatorial position. They and others (James et al., 1976) have argued that in this arrangement C5H becomes a better leaving group and the Cys 146 sulfur a worse leaving group, thereby favoring the desired elimination.

We have been unable to fit a model of the isomerized ligands into any of the known TS conformations without disrupting the normally occurring protein−ligand contacts. The difficulty lies in placing Cys 146 in the equatorial position, which simply cannot be accommodated without severe changes in the active site geometry. In addition, we have shown that the dUMP−Cys 146 covalent bond is unstable and disappears with relatively minor changes in the active site geometry (Weichsel & Montfort, unpublished results). We therefore have searched for other models consistent with the observed TS ligand arrangements and correct stereochemistry.

[2] Numbering: Residue numbers for *E. coli* TS are used throughout the paper. The conversion to *L. casei* TS numbering is as follows: $I + 2$ for $I \leq 87$, $I + 52$ for $I > 87$. Amino acids from one monomer that appear in the active site of the other monomer are indicated by a prime, as in 126′. Ordered water molecules are numbered and named according to the residue with which they are associated (e.g. Wat_2E58 is the second water bound to Glu 58).

As noted above, the arrangement we found in the present structures has C5F *gauche* to THF, which is therefore not aligned for an E2 elimination that retains the known stereochemistry. In addition, the fluorine at C5 is in a pseudoequatorial position (Figure 4). As argued above, it seems unlikely that the ligands could obtain a conformation with orbitals aligned for concerted E2 elimination. However, if the elimination took place in two distinct steps, starting with removal of C5H, major changes in ligand or active site geometry would not be required. The E1CB mechanism for elimination fits these parameters, as previously discussed (Finer-Moore et al., 1990), and would give rise to products of correct stereochemistry without isomerization of the ligands (discussed below).

The factors that favor an E1CB mechanism are: (i) a poor second leaving group, (ii) a means of stabilizing the carbanion intermediate, and (iii) an acidic proton. The 5-amine of THF is indeed a poor leaving group, and the carbanion intermediate can be stabilized through conjugation with the pyrimidine ring, but the C5 proton is in a pseudoequatorial position, which would make it less acidic than if it were pseudoaxial, where conjugation between the developing carbanion and C4 carbonyl could occur. That such an equatorial proton could be more acidic than expected has been demonstrated in a study of bridgehead carbanions derived from bicyclic piperazinediones (Williams et al., 1983). However, a possibly more important factor in increasing the acidity of the C5 proton is the unstable Cys 146−C6 conjugate, as discussed in the next two sections.

Strain on the Thiol Adduct Leads to Bond Instability. The TS thiol adduct appears to be unstable. Numerous structures of TS bound to dUMP, FdUMP, or dTMP and a folyl analogue have revealed the occurrence of this bond to be highly variable (Weichsel & Montfort, 1995; Matthews et al., 1990a; Weichsel & Montfort, unpublished results). This is also the case in the present structures (Figure 5). The reason appears to be the tightly restrained positions for Cys 146 and dUMP in the TS active site and favorable electrostatic interactions for the thiolate anion (Figure 4). Cys 146 is restrained through hydrogen bonding to Tyr 94 (C146 N−Y94 OH, 2.7 Å in the trigonal structure) and Arg 166 (C146 O−R166 N, 3.1 Å, not shown), which is the terminal hydrogen bond in two strands of the core β sheet. The Cys 146 containing bulge is further restrained through hydrogen bonds between the carbonyl of Pro 145 and R166 Nϵ (3.1 Å) and the carbonyl of Ala 144 and R166 NH1 (2.9 Å). Arg 166 is further restrained in the ternary complex by two hydrogen bonds to the nucleotide phosphate oxygens (2.7 Å each) and to the carbonyl of Arg 126′ (2.8 Å). In addition, the guanidinyl group of Arg 166 and the sulfur of Cys 146 are in van der Waals contact. Thus, any movement of Cys 146 is transmitted through Arg 166 to the nucleotide.

An additional 10 hydrogen bonds are formed between FdUMP and TS in the present structures, as was previously found in crystal structures containing nucleotide and the folyl analogue CB3717 (Montfort et al., 1990; Matthews et al., 1990a). Five of these anchor FdUMP to the active site wall opposite Cys 146. The TS ligand-induced conformational change serves to bring the two sides of the active site closer together such that Cys 146 and C6 of the pyrimidine ring can react (Roberts & Montfort, unpublished results). Rotation of the nucleotide ring is further restrained through extensive stacking with the folyl pterin ring. That the covalent adduct occurs during catalysis is not in disupute. It appears, however, that the tightly restrained positions of the reacting groups oppose formation of an optimal covalent bond, resulting in a bond that never becomes more than marginally stable.

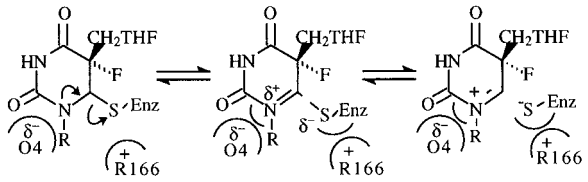

FIGURE 7: Possible mechanism leading to thiol adduct instability for the FdUMP-containing analogue to intermediate **III**. Strain on the Cys 146−C6 bond favors electron withdrawal from the pyrimidine ring, leading to charge separation between N1 and the Cys 146 sulfur. A polarized thiol adduct (middle structure) would lead to partial charge separation, and a completely broken bond (right-hand structure) to full charge separation. Nearby ionic groups (shown in half circles) would serve to stabilize the ionic species. The ternary complex crystals may contain a mixed population of these three states, leading to the poorly defined electron density in this region.

A possible mechanism leading to the poor electron density at C6 in the present structures is shown in Figure 7. Three states are illustrated: fully linked, partially linked, and unlinked. The fully linked state is analogous to the intermediate previously proposed by Santi and co-workers (intermediate **III** of Figure 1). The present structures may contain a mixed population of these three states and thus multiple positions for C6 (through rehybridization), which could account for the poor electron density observed. That imminium ion formation may occur through a double bond between N1 and C6, rather than between N1 and C2 where oxyanion formation could stabilize the imminium ion, is suggested by the observed electron density. The physical restrictions placed on the thiol adduct by the enzyme may be sufficient to polarize the bond, generate a partial charge separation between C6 and the Cys 146 sulfur, and attract the N1 lone pair electrons. Electrostatic interactions in the active site are in a position to stabilize the resulting charge separation: the anionic form of Cys 146 is stabilized by Arg 166, and the developing positive charge on N1 stabilized by the partial negative charge at O4 of THF (indicated by half circles in Figure 7). Sulfide stabilization of the imminium ion may also occur (LaLonde, 1980; LaLonde & Eckert, 1983). Chemical precedence for the imminium ion shown in Figure 7 comes from studies of *N*-acyliminium ion cyclizations (Speckamp et al., 1994; Udding et al., 1994).

An alternative explanation for the poor density at C6 is that, since the C5 fluorine cannot be extracted by the enzyme, some percentage of the complexes in the crystal have eliminated both CH_2THF and Cys 146 (giving rise to either the 5 imminium ion of intermediate **II** or some derivative of this intermediate, and FdUMP of intermediate **I**). We disfavor this possibility since there is no sign of CH_2THF elimination in the electron density maps, and poor density at C6 similar to the present results has been seen in other complexes (Weichsel & Montfort, unpublished results). It should also be noted that, due to the strong electron-withdrawing potential of fluorine, the thiol adduct would be expected to be *more* stable in the FdUMP complex than in the dUMP complex, which would argue that the true intermediate **III** has an even weaker thiol adduct than that seen in our current structures.

A Polar Thiol Adduct Leads to Increased Acidity for C5H. The proposed polar thiol adduct would lead to increased acidity for C5H in three ways. First, the electron-withdrawing effect of a full or partial positive charge at N1 would stabilize negative charge buildup at C5 and facilitate hydrogen abstraction. Second, with the restrictions at C6 due to thiol addition reduced or removed, C5 would have more freedom to alter its geometry, allowing the C5 hydrogen to move toward the pseudoaxial position and thus become more acidic. Model building suggests that the relatively small adjustments in the ring position and ring geometry required to move this hydrogen toward an axial position are readily accommodated if the Cys 146 thiolate is not required to also shift to an equitorial position (see, for example, intermediate **IV** in Figure 6). Third, proton abstraction with Cys 146 either partially or fully eliminated would lead to increased aromaticity for the pyrimidine ring and an accompanying resonance stabilization energy. Taken together, these three factors would serve to increase the acidity of the C5 hydrogen.

C5H Abstraction May Involve Tyr 94. An essential step in the breakdown of intermediate **III** is the abstraction of the proton from position 5 of the pyrimidine ring by an active site base, and the nature of this base has been the subject of considerable debate. Three potential bases lie near C5F in the present structure: the hydroxyl of Tyr 94, water Wat_2E58, and water Wat_1Y94 (Figure 4). Both waters have been suggested as candidates for the base, either alone (Matthews et al., 1990b; Fauman et al., 1994) or as a conduit to N5 of THF (Hardy et al., 1995). In the present structures, the pseudoequatorial C5F is in van der Waals contact with the Tyr 94 hydroxyl (3.2 Å) and in an optimal configuration for proton abstraction via an E1CB mechanism. We have recently demonstrated that the mutant protein Tyr 94 → Phe is nearly devoid of catalytic activity yet quickly accumulates a covalent complex that contains TS, dUMP, and CH_2THF (Maley, unpublished data). A likely candidate for this complex is intermediate **III**, the intermediate immediately preceding proton abstraction. The crystal structure of this mutant complexed with dUMP and CB3717 is nearly identical to the wild type structure, except for a slightly less prevalent thiol adduct and a shift of water Wat_1Y94 toward C5 of dUMP, where it could substitute for the hydroxyl of Y94 (Weichsel & Montfort, unpublished results). These data are consistent with Tyr 94 being the base for C5H abstraction.

For tyrosine to be an effective base, it should have a pK_a reduced from its normal value of about 10 to a value closer to neutral pH. A strong hydrogen bond to the amide of Cys 146 (2.7 Å) and a hydrogen bond to ordered water Wat_1Y94 (2.9 Å) may serve to lower the pK_a to a sufficient degree for catalysis, although it seems unlikely to yield a pK_a of 7.5. That the anionic form of Tyr 94 is readily formed is supported by the covalent addition of 5-(trifluoromethyl)-dUMP to the equivalent tyrosine (Tyr 146) of *L. casei* TS (Eckstein et al., 1994). The proposed mechanism for this addition involves nucleophilic attack by the tyrosine hydroxylate anion.

*Intermediate **IV** Is Consistent with the Known Stereochemistry.* Abstraction of C5H from the conformation observed in the present crystal structures would yield a configuration for intermediate **IV** that is consistent with the known stereochemistry for hydride transfer. The energy-minimized model for this intermediate is shown in Figure 6. In our model for intermediate **IV**, the bond between N5 and C11 has rotated approximately 120° from its position in intermediate **III** (represented by the present structure, Figure 4) and is in a stereochemically correct orientation for hydride transfer. This rotation is a consequence of the rehybridization of C5 to sp^2 upon double bond formation. N5 of THF is further pyramidalized to accommodate the change in geometry at C5 of the pyrimidine. Except for rotation of the methylene bridge, only small shifts in the ligands, and no shifts in the protein, are required to reach this conformation. All ligand−protein contacts are maintained in the model.

Elimination of THF(Elimination Step 2) and Hydride Transfer. The geometry of our model for intermediate **IV** is such that direct hydride transfer could displace THF from C11 (Figure 6). Studies with model compounds, however, strongly favor a mechanism that proceeds in distinct steps involving an exocyclic methylene, shown as intermediate **V** in Figure 1 [reviewed in Pogolotti and Santi (1977)]. Model building suggests intermediate **V** is readily accommodated in the TS active site and H6 of THF optimally placed for hydride transfer (Figure 6).

Protonation of N5 would make THF a much better leaving group, and it has been suggested that the elimination step may be acid catalyzed. The increased pyramidalization of N5 we found in modeling of intermediate **IV** would increase its basicity (with respect to intermediate **III**) and make it more readily protonated. However, the identity of an appropriate acid is not readily apparent from inspection of the TS active site. Matthews and co-workers (1990b) suggested the proton could be donated from O4 of THF, or from an intervening solvent molecule associated with O4, in a mechanism involving stabilization of the protonated form of O4 through hydrogen bonding between N3 and Asp 169. Such a mechanism would require stabilization of the anionic form of Asp 169, since the residue is buried in the ternary complex. Alternatively, protonation could occur through one of the ordered solvent molecules in the complex. Wat_1E58, which is hydrogen bonded to N10, is 4.1 Å from N5 in the present structures and 3.7 Å away in the model of intermediate **IV**, and thus could protonate N5. Once THF was eliminated, N5 would rehybridize to sp^2, increasing its acidity through conjugation with the pterin rings. This increase in acidity would facilitate the subsequent deprotonation of N5 and hydride transfer, as shown in Figure 1.

Mechanisms Involving the Polar Thiol Adduct. Figure 8 summarizes two possible pathways for breakdown of intermediate **III** that are consistent with an unstable C6−Cys 146 bond. In Figure 8a, the thiol adduct is polarized but remains in place until the final step. In Figure 8b, the thiol adduct breaks before proton abstraction or elimination of THF, giving rise to intermediate **IIIc**. Both **IIIb** and **IIIc** would result in increased acidity for the C5 proton, as discussed above. The charges that develop at N1 and Cys 146 in these pathways would be stabilized through ionic interactions with Arg 166 and folate (Figure 7). Hydride transfer would be facilitated by the charge separation present in intermediates **Vb** or **Vc**. Only small conformational changes from the models in Figure 6 are required for either of these pathways, and both give rise to the correct stereochemistry for product formation.

Conformational Change during Catalysis. The role of ligand-induced conformational change in catalysis by non-

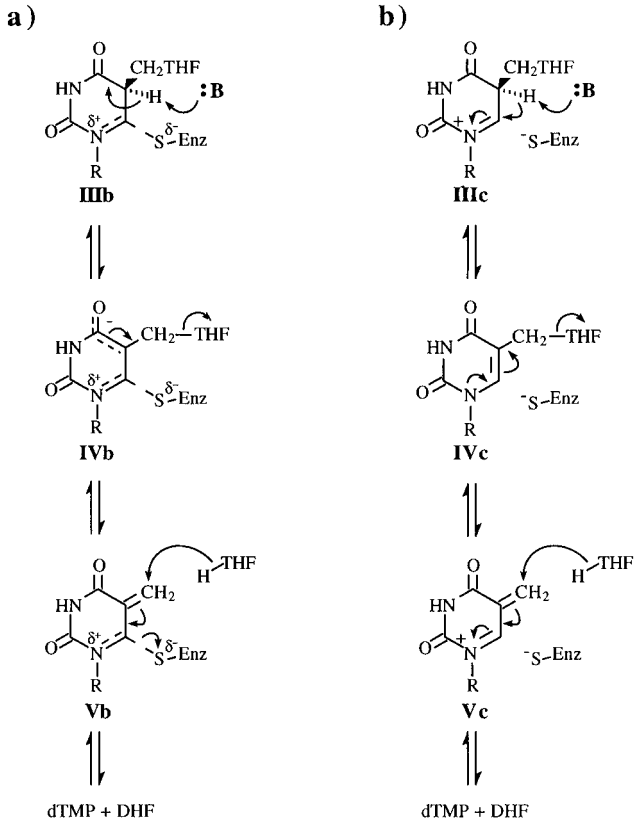

FIGURE 8: Two variations in our proposed mechanism for breakdown of the covalent ternary complex. In both cases strain on the C6−Cys 146 bond increases the acidity of C5H by withdrawing electrons from the pyrimidine ring. (a) The reaction proceeds from an intermediate with a strained thiol adduct. (b) The reaction proceeds from an intermediate in which the C6−Cys 146 bond has broken. The hydride transfer step is assisted by either a partial (**Vb**) or full (**Vc**) positive charge at N1.

allosteric enzymes is much debated but still poorly understood [see for example Gerstein et al. (1994)]. Described in this section are several consequences of the TS conformational change and the possible advantages of incorporating such changes into the TS catalytic mechanism.

The most obvious consequence of the conformational change is that the ligands become almost completely buried. Extensive contacts between protein and ligands ensure that reactive intermediates are well aligned for reaction with one another, but screened from bulk solvent. The reactive nucleophile at C5 of dUMP and reactive electrophile at C11 of CH_2THF are not generated until both substrates are in place [CH_2THF does not bind in the absence of nucleotide (Galivan et al., 1976b), and dUMP binds to the open conformation (Roberts & Montfort, unpublished results)]. To achieve this protection, TS must have an open conformation for substrate binding and product release and a closed conformation during catalysis.

We argue above that TS destabilizes the thiol adduct with nucleotide through extensive ligand contacts, resulting in a polarized bond and increased acidity for the C5 proton. The TS conformational flexibility may further strain this bond since the open conformation appears to be the more stable in the absence of ligands, resulting in a constant force opposing the closed conformer and the thiol adduct. These factors also appear to block formation of the trans diequatorial conformation of intermediate **III**, which is quite stable in the absence of protein (James et al., 1976). Thus, the same features that give rise to the observed polar thiol adduct may also prevent formation of a stable reaction intermediate that would impede catalysis.

The enclosure of substrates in the TS active site may help overcome one of the chief obstacles to catalysis: the difficulty in binding a high-energy, transition-state-like ligand conformation that, by definition, is at much lower concentration in solution than other conformations of the ligand (Wolfenden, 1974). The open TS conformation allows dUMP binding but keeps Cys 146 away from C6. Modeling studies suggest the CH_2THF extended conformation can also loosely bind to the open TS conformation through electrostatic interactions (between Lys 48, Arg 49, His 51, Lys 259, and the folyl glutamate) and hydrophobic interactions (between Ile 79, Trp 80, Trp 83, Phe 176, dUMP, and the folyl pterin and PABA rings). Such interactions with the open protein conformation would allow binding to occur at every encounter of substrate and protein. Enclosure of substrates after initial binding would lead to a large number of protein−ligand contacts, stabilization of the higher energy conformation of CH_2THF, and catalysis of ring opening. Initial binding would be greater for the polyglutamylated form of the cofactor, as occurs *in vivo* (Matthews et al., 1987), through increased electrostatic interactions. That the glutamate portion of the cofactor is important for binding has been demonstrated with cofactor analogues containing modified glutamates, which are very poor substrates for TS (Slavik & Zakrzewski, 1967).

Thus, we propose that the TS conformational change serves five functions: (i) it allows binding of ligands in their ground-state conformers; (ii) it provides a means for stabilizing the higher energy "bent" conformer of CH_2THF; (iii) it prevents the reactive intermediates from occurring until they are in a position to react with one another; (iv) it actively assists in catalysis by straining the Cys 146−dUMP thiol adduct to help generate polar bonds at N1 and C6 and increase the acidity of C5H; and (v) it helps prevent the thiol adduct from adopting a stable conformation and falling into a "thermodynamic hole".

CONCLUSIONS

Structural and chemical data concerning the six potential intermediates illustrated in Figure 1 are needed to understand the TS mechanism. Recently, structures of the product complex (intermediate **VI** (Weichsel & Montfort, unpublished results; Fauman et al., 1994)), and numerous analogues of intermediates **I** and **II**, have been determined [reviewed in Carreras and Santi (1995); Weichsel & Montfort, unpublished results]. Structures closely analogous to intermediate **III** were the subjects of Matthews et al. (1990b) and the present study. Structural data concerning intermediates **IV** and **V** are still lacking, but based on the present results and the assumption that all major TS conformations are known, we have modeled these intermediates, as well as intermediates **I** and **II**. The key conclusions from this are (1) the TS eliminations occur in a stepwise manner with abstraction of C5H preceding THF elimination; (2) the Cys 146 sulfur remains axial to the nucleotide ring throughout catalysis; (3) TS uses strain and electrostatic interactions to polarize or break the sulfur adduct to C6 during catalysis, which increases the acidity of C5H in three ways; (4) the TS ligand-induced conformational change provides a means for binding

high-energy substrate conformations and plays an active role in catalysis; and (5) the likely base for removal of C5H is Tyr 94.

Two possible mechanisms incorporating these conclusions are shown in Figure 8, one in which the Cys 146 bond is polarized but remains in place and one in which the Cys 146 bond breaks before abstraction of the proton from C5. We cannot at present determine which of these two pathways is more likely to be correct. Rather, our intent is to suggest that the poor quality of the thiolate bond contributes to the acidity of C5H, facilitating its removal, and contributes to the electrophilicity of the exocyclic methylene at C5 of intermediate **V**, facilitating hydride transfer and the completion of the catalytic cycle. Such a mechanism is consistent with the known TS conformations and does not require a large change in ligand or protein geometry once the productive complex has been formed, unlike previously proposed mechanisms (James et al., 1976; Matthews et al., 1990b).

ACKNOWLEDGMENT

We are indebted to Professors Jacquelyn Gervay and Richard Glass for insightful discussions concerning our proposed mechanism.

REFERENCES

Byrd, R. A., Dawson, W. H., Ellis, P. D., & Dunlap, R. B. (1978) *J. Am. Chem. Soc. 100*, 7478−7486.

Carreras, C. W., & Santi, D. V. (1995) *Annu. Rev. Biochem. 64*, 721−762.

Collaborative Computational Project, Number 4. (1994) *Acta Crystallogr. D50*, 760−763.

Eckstein, J. W., Foster, P. G., Finer-Moore, J., Wataya, Y., & Santi, D. V. (1994) *Biochemistry 33*, 15086−15094.

Elden, S., & Jencks, W. P. (1996) *J. Am. Chem. Soc. 117*, 4851−4857.

Fauman, E. B., Rutenber, E. E., Maley, G. F., Maley, F., & Stroud, R. M. (1994) *Biochemistry 33*, 1502−1511.

Finer-Moore, J., Fauman, E. B., Foster, P. G., Perry, K. M., Santi, D. V., & Stroud, R. M. (1993) *J. Mol. Biol. 232*, 1101−1116.

Finer-Moore, J. S., Montfort, W. R., & Stroud, R. M. (1990) *Biochemistry 29*, 6977−6986.

Furey, W., Wang, B. C., & Sax, M. (1982) *J. Appl. Crystallogr. 15*, 160−166.

Galivan, J. H., Maley, G. F., & Maley, F. (1976a) *Biochemistry 15*, 356−362.

Galivan, J. H., Maley, F., & Baugh, C. M. (1976b) *Biochem. Biophys. Res. Commun. 71*, 527−534.

Gerstein, M., Lesk, A. M., & Chothia, C. (1994) *Biochemistry 33*, 6739−6749.

Hardy, L. W. (1995) *Acta Biochim. Pol. 42*, 367−380.

Hardy, L. W., & Nalivaika, E. (1992) *Proc. Natl. Acad. Sci. U.S.A. 89*, 9725−9729.

Hardy, L. W., Graves, K. L., & Nalivaika, E. (1995) *Biochemistry 34*, 8422−8432.

Huang, W., & Santi, D. V. (1994) *J. Biol. Chem. 269*, 31327−31329.

Insight II version 2.2.0, Biosym Technologies (1993), San Diego, CA.

James, T. L., Pogolotti, A. L., Ivanetich, K. M., Wataya, Y., Lam, S. S. M., & Santi, D. V. (1976) *Biochem. Biophys. Res. Commun. 72*, 404−410.

Jones, T. A. (1978) *J. Appl. Crystallogr. 11*, 268−272.

Jones, T. A., Zou, J. Y., Cowan, S. W., & Kjelgard, M. (1991) *Acta Crystallogr. A47*, 110−119.

Kabsch, W. (1988) *J. Appl. Crystallogr. 21*, 916−934.

Kallen, R. G., & Jenks, W. P. (1966) *J. Biol. Chem. 241*, 5851−5863.

Kamb, A., Finer-Moore, J. S., & Stroud, R. M. (1992) *Biochemistry 31*, 12876−12884.

Kraulis, P. J. (1991) *J. Appl. Crystallogr. 24*, 946−950.

LaLonde, R. T. (1980) *Acc. Chem. Res. 13*, 39−44.

LaLonde, R. T., & Eckert, T. S. (1983) *J. Org. Chem. 48*, 3841−3842.

Leary, R. P., Gaumont, Y., & Kisliuk, R. L. (1974) *Biochem. Biophys. Res. Commun. 56*, 484−488.

Lu, Y.-Z., Aiello, P. D., & Matthews, R. G. (1984) *Biochemistry 23*, 6870−6876.

Maley, G. F, & Maley, F. (1988) *J. Biol. Chem. 263*, 7620−7627.

Matthews, D. A., Appelt, K., Oatley, S. J., & Xuong, N. H. (1990a) *J. Mol. Biol. 214*, 923−936.

Matthews, D. A., Villafranca, J. E., Janson, C. A., Smith, W. W., Welsh, K., & Freer, S. (1990b) *J. Mol. Biol. 214*, 937−948.

Matthews, R. G., Ghose, C., Green, J. M., Matthews, K. D., & Dunlap, R. B. (1987) *Adv. Enz. Reg. 26*, 157−171.

Messerschmidt, A., & Pflugrath, J. W. (1987) *J. Appl. Crystallogr.* 20, 306−315.

Montfort, W. R., Perry, K. M., Fauman, E. B., Finer-Moore, J. S., Maley, G. F., Hardy, L., Maley, F., & Stroud, R. M. (1990) *Biochemistry 29*, 6964−6977.

Pflugrath, J. W., Saper, M. A., Quiocho, F. A. (1984) in *Methods and Applications in Crystallographic Computing* (Hall, S., & Ashida, T., Eds.) pp 404−407, Clarendon Press, Oxford.

Poe, M., Jackman, L. M., & Benkovic, S. J. (1979) *Biochemistry 18*, 5527−5530.

Pogolotti, A. L., Jr., & Santi, D. V. (1977) *Bioorg. Chem. 1*, 277−311.

Santi, D. V., & Danenberg, P. V. (1984) in *Folates and Pterins* (Blakely, R. L., & Benkovic, S. J., Eds.) Vol. 1, Chemistry and Biochemistry of Folates, pp 345−398, Wiley, New York.

Santi, D. V., McHenry, C. S., Raines, R. T., & Ivanetich, K. M. (1987) *Biochemistry 26*, 8606−8613.

Santi, D. V., McHenry, C. S., & Sommer, H. (1974) *Biochemistry 13*, 471.

Slavik, K., & Zakrzewski, S. F. (1967) *Mol. Pharmacol. 3*, 370−377.

Sliecker, L. J., & Benkovic, S. J. (1984) *J. Am. Chem. Soc. 106*, 1833−1838.

Smith, I., Jones, A., Spielmann, M., Namer, M., Green, M. D., Bonneterre, J., Wander, H. E., Hatschek, T., Wilking, N., Zalcberg, J., Spiers, J., & Seymour, L. (1996) *Br. J. Cancer 74*, 479−481.

Smith, G. K., Amyx, H., Boytos, C. M., Duch, D. S., Ferone, R., & Wilson, H. R. (1995) *Cancer Res. 55*, 6117−6125.

Sommer, H., & Santi, D. V. (1974) *Biochem. Biophys. Res. Commun. 57*, 689−695.

Speckamp, W. N., Newcombe, N. J., Hiemstra, H., Ya, F., Vijn, R. J., & Koot, W.-J. (1994) *Pure Appl. Chem. 66*, 2163−2166.

Stout, T. J., & Stroud, R. M. (1996) *Structure 4*, 67−77.

Tamelen, E. E., & Hopla, R. E. (1979) *J. Am. Chem. Soc. 101*, 6114−6115.

Tatum, C., Vederas, J., Slieker, E., Benkovic, S. J., & Floss, H. (1977) *J. Chem. Soc., Chem. Commun.* 218−220.

Udding, J. H., Papin, N., Hiemstra, H., & Speckamp, W. N. (1994) *Tetrahedron 50*, 8853−8862.

Webber, S., Bartlett, C. A., Boritzki, T. J., Hillard, J. A., Howland, E. F., Johnston, A. L., Kosa , M., Margosiak, S. A., Morse, C. A., & Shetty, B. V. (1996) *Cancer Chemother. Pharmacol. 37*, 509−517.

Weichsel, A., & Montfort, W. R. (1995) *Nature Struct. Biol. 2*, 1095−1101.

Weichsel, A., Montfort, W. R., Ciesla, J., & Maley, F. (1995) *Proc. Natl. Acad. Sci. U.S.A. 92*, 3493−3497.

Williams, R. M., Dung, J.-S., Josey, J., Armstrong, R. W., & Meyers, H. (1983) *J. Am. Chem. Soc. 105*, 3214−3220.

Wolfenden, R. (1974) *Mol. Cell. Biochem. 3*, 207−211.

Zapf, J. W., Weir, M. S., Emerick, V., Villafranca, J. E., & Dunlap, R. B. (1993) *Biochemistry 32*, 9274−9281.

BI962936J